Cancer Chemother Pharmacol (2011) 68:389–398
DOI 10.1007/s00280-010-1495-6

ORIGINAL ARTICLE

The histone deacetylase inhibitor PXD101 increases the efficacy of irinotecan in in vitro and in vivo colon cancer models

Young-Soon Na · Kyung-Ah Jung · Seung-Mi Kim · Yong Sang Hong · Min-Hee Ryu · Se Jin Jang · Dae Hyuk Moon · Dong-Hyung Cho · Jin Cheon Kim · Jung Shin Lee · Tae Won Kim

Received: 22 June 2010 / Accepted: 8 September 2010 / Published online: 3 November 2010

Abstract
Purpose Histone deacetylase inhibitors (HDACIs), such as PXD101 and suberoylanilide hydroxamic acid, inhibit proliferation and stimulate apoptosis of tumor cells. The enhanced effectiveness of chemotherapy or radiotherapy when combined with HDACIs has been observed in several cancers. In this study, we investigated the antitumor effect of PXD101 combined with irinotecan in colon cancer.
Methods HCT116 and HT29 colon cancer cells for cell viability assay were treated with PXD101 and/or SN-38, the active form of irinotecan. Antitumor effects of HCT116 and HT29 xenografts treated with these combinations were evaluated. [^{18}F]FLT-PET was used to detect early responses to PXD101 and irinotecan in colon cancer.
Results PXD101 and SN38 possessed dose-dependent antiproliferative activity against HCT116 and HT29 cells and exerted a synergistic effect when used in combination. In xenografted mice, PXD101 in combination with irinotecan dramatically inhibited tumor growth without causing additive toxicity. Apoptotic effects on xenograft tumors were greater with combined treatment than with irinotecan alone. [^{18}F]FLT-PET imaging revealed a 64% decrease in [^{18}F]FLT uptake in tumors of HCT116 xenograft-bearing mice treated with a combination of PXD101 and irinotecan, indicating a decrease in thymidine kinase 1 (TK1) activity. These results were supported by Western blot analyses showing a decrease in tumor thymidine kinase 1 protein levels, suggesting that [^{18}F]FLT-PET can be used to non-invasively detect early responses to these agents.
Conclusions These data show that PXD101 increases the cytotoxic activity of irinotecan in in vitro and in vivo colon cancer models and suggest these agent combinations should be explored in the treatment of colon cancer.

Keywords Histone deacetylase inhibitor · PXD101 · Irinotecan · [^{18}F]FLT-PET · Colon cancer

Y.-S. Na · K.-A. Jung · S.-M. Kim · D.-H. Cho
Institute for Innovate Cancer Research,
Asan Medical Center, Seoul, Korea

Y. S. Hong · J. S. Lee · T. W. Kim (✉)
Department of Oncology, Asan Medical Center,
University of Ulsan College of Medicine,
Institute for Innovate Cancer Research,
86 Asan Byungwon Gil, Songpa-gu, Seoul 138-736, Korea
e-mail: twkimmd@amc.seoul.kr

M.-H. Ryu
Department of Oncology, Asan Medical Center,
University of Ulsan College of Medicine, Seoul, Korea

S. J. Jang
Department of Pathology, Asan Medical Center,
University of Ulsan College of Medicine,
Institute for Innovate Cancer Research, Seoul, Korea

D. H. Moon
Department of Nuclear Medicine, Asan Medical Center,
University of Ulsan College of Medicine,
Institute for Innovate Cancer Research, Seoul, Korea

J. C. Kim
Department of Surgery, Asan Medical Center,
University of Ulsan College of Medicine,
Institute for Innovate Cancer Research, Seoul, Korea

Introduction

Colorectal cancer is the second leading cause of cancer-related deaths in the western world [1]. In recent years, novel biological agents, including bevacizumab and cetuximab, when added to conventional 5-fluorouracil (5-FU) and irinotecan or oxaliplatin treatment regimens have improved efficacy in patients

with advanced colorectal cancer [2]. However, if these agents fail, there are no effective alternatives; thus, there is a clear need for new therapeutic approaches.

Irinotecan (Campto®) is an effective chemotherapeutic agent for colorectal cancer [3] and a prodrug that is activated to the topoisomerase I inhibitor SN-38 by intracellular carboxylesterases. Topoisomerase I makes a single-strand break in DNA during replication and then relegates the broken strands. SN38 traps these DNA strand breaks and induces formation of replication-mediated double-strand breaks. Therefore, SN-38 leads to inhibition of DNA replication and transcription [3, 4].

Histone deacetylase inhibitors (HDACIs) have recently emerged as a class of anticancer agents. HDACIs cause growth arrest via a mechanism that involves induction of p21 and downregulation of cyclins. They also induce apoptosis and autophagy, modulate reactive oxygen species-facilitated cell death by promoting thioredoxin degradation, and prevent angiogenesis [5]. HDACI valproic acid (VPA) has shown cell-type-specific effects on cell migration, proliferation [6], and Erk1/2 activity [7, 8].

PXD101 (Belinostat) is a novel, low molecular weight hydroxamic acid HDACI, and is currently being investigated in patients with advanced solid tumors. Evidence to date indicates that specific histone deacetylases (HDACs), including HDAC 1, 2, 3, and 8, are consistently overexpressed in colon cancer [9–11]. Inhibition of these proteins by HDACIs revealed the antiproliferative effect on colon cancer cells in vitro and in vivo [12, 13], thus confirming this upregulation is functionally significant. Moreover, HDACIs have been shown to synergize with well-established chemotherapeutic agents to enhance antitumor effects in colon cancer [14, 15]. Therefore, we investigated the antitumor effect of HDACi combined with irinotecan because of facilitating actions that the action of HDACi may enhance the action of irinotecan.

As the clinical evaluation of HDACIs continues, the role of biomarkers in identifying responsive patients and evaluating treatment responses becomes increasingly important. To date, a few biomarkers capable of predicting the response to HDACIs have been established in vitro [16, 17]. Recently, it has been suggested that non-invasive imaging with 3′-deoxy-3′-[^{18}F]fluorothymidine ([^{18}F]FLT) positron emission tomography (PET) could be used to predict and monitor responses to chemotherapy in tumors [18], and [^{18}F]FLT used as a radiotracer can assess tumor cell proliferation. Results from [^{18}F]FLT-PET studies have shown that because [^{18}F]FLT is a substrate for thymidine kinase 1 (TK1), [^{18}F]FLT uptake in tumors represents TK1 protein levels [19, 20].

In this study, we demonstrated that the combination of PXD101 with irinotecan synergistically enhances cell killing in vitro and inhibits tumor growth in a xenograft model of colon cancer, producing an antitumor effect greater than either agent alone. The response of patients with colon cancer to PXD101 could be predicted using [^{18}F]FLT as an imaging biomarker. Collectively, these data suggest that combining PXD101 with irinotecan is a promising novel therapeutic strategy for treating colon cancer.

Materials and methods

Cell lines, compounds, and antibodies

The human colon cancer cell lines HCT116 and HT29 were obtained from the American Type Culture Collection (Manassas, VA). PXD101 was obtained from CrystalGenomics (Seoul, Korea). Irinotecan and SN-38 were obtained from Pfizer Korea Inc. (CT, USA) and Hanmi Pharmaceuticals (Seoul, Korea), respectively. For Western blot analyses, primary antibodies against acetyl-H3, H3, p21 (Cell Signaling, Danvers, MA), XIAP (BD Biosciences, San Jose, CA), TK1 (Abnova, Taipei, Taiwan), and β-actin (Santa Cruz Biotechnology, Santa Cruz, CA), and secondary antibodies conjugated with horseradish peroxidase were used.

Cell viability assay and analysis of drug combination effects

Cell viability was determined using a Cell Counting Kit-8 (Dojindo Laboratories, Kumamoto, Japan) according to the manufacturer's instructions. Three independent experiments were performed in duplicate. Cell viability curves were plotted as change relative to untreated cells, and IC_{50s} were determined using GraphPad Prism (Graphpad Software Inc., San Diego). A combination index (CI) was calculated according to the Chou-Talalay equation [21, 22] using CalcuSyn software (Biosoft, Cambridge, UK). A combination index value <1 indicates synergy; a CI value = 1 indicates an additive effect; and a CI value >1 indicates antagonism. The interaction between PXD101 and SN38 was assessed at concentrations of IC_{20} followed by 1.5-fold increasing or decreasing for each cell line.

Cell-cycle analysis, annexinV staining, and soft agar colony-forming assay

The cell-cycle distribution was analyzed by flow cytometry (Becton–Dickinson, Franklin Lakes, NJ) and Cell Quest software (BD) using propidium iodide (PI; Molecular Probes, Leiden, Nederlands)-stained cells. The percentage of early apoptotic cells detected by measuring Annexin V protein of cell membrane in cancer cells exposed for 48 h to PXD101 or SN38 alone or in combination was determined using an annexin V-FITC apoptosis detection kit (BD Biosciences) and flow cytometry according to the manufacturer's

protocol. Results represented the mean ± SEM of three independent experiments as percentages of Annexin V positive and PI-negative cells. A soft agar colony-formation assay was performed using a CytoSelect 96-Well Cell Transformation Assay (Cell Biolabs, San Diego, CA) as recommended by the manufacturer.

Xenograft model

Five-week-old female athymic nude (nu/nu) mice were purchased from Japan SLC Inc. (Shizuoka, Japan). Tumors were established by injecting 5×10^6 colon cancer (HCT116 and HT29) cells subcutaneously into the left flank of mice. When subcutaneous tumors reached a size of 100 mm^3 (day 0), xenografted animals were randomly allocated into one of the following four groups: Control (vehicle treated: 520 mM L-arginine (pH 9.4)), PXD101 only, Irinotecan only, and PXD101 and irinotecan. PXD101 (60 mg/kg) was administered once daily for 5 days followed by 2 days without treatment; this cycle was repeated for 3 weeks. Irinotecan was administered at a dose of 50 mg/kg once weekly for 3 weeks. The PXD101/irinotecan combination group was administered PXD101 in the morning followed by irinotecan in the afternoon for 3 weeks when both drugs were injected. Drug and vehicle were administered intraperitoneally (i.p.). Tumors were measured by caliper twice weekly and calculated as volume (mm^3) = (length × $width^2$)/2. Body weights were also monitored. On days 2 and 16, specimens of tumors were collected for soft agar assay, TUNEL assay, or Western blotting. This study was approved by the Institutional Animal Care and Use Committee (IACUC).

Isolation of primary tumor cells and preparation of tumor tissue extracts

The tumor tissue pieces were filtered through a 100-μm cell strainer (BD Biosciences) to remove tissue fragments. Cells were centrifuged and washed for soft agar assay. The dissected tumors were homogenized in tissue lysis buffer (50 mM Tris–HCl (pH 8.0), 150 mM NaCl, 0.02% sodium azide, 0.1% SDS, 1% NP-40, 0.5% sodium deoxycholate, 10 μl/ml protease inhibitor mix). Homogenates were centrifuged and then analyzed by Western blotting.

TUNEL staining and hematoxylin–eosin staining

Tumor tissues were isolated on day 2 and day 16, and fixed in 10% phosphate-buffered formalin, paraffin-embedded, and sectioned into 4-μm-thick section. Apoptosis was determined by TUNEL staining using an In Situ Cell Death Detection Kit (Roche-Applied Science, Indianapolis, IN) as described by the manufacturer. Sections were counter-stained with 4′-6-diamidino-2-phenylindole (DAPI) to stain nuclei. Three independent fields in each slide were analyzed at high power under a fluorescence microscope. Signals were quantified using Image J software (NIH). The basic histomorphological features of organs were evaluated by hematoxylin–eosin (H&E) staining of tumor specimens collected on day 9 from agent-treated, xenograft-bearing mice.

[^{18}F]-FLT PET imaging

[^{18}F]-FLT was prepared according to a previously reported method [23]. PET images were obtained 2 h after intravenous injection of each PET tracer (37 MBq/mouse). The total acquisition time was 10 min. Xenografts were randomized into four groups, as described earlier, and then a standardized uptake value (SUV) for basal TK1 levels was determined by PET on day 0. HCT116 xenografts were treated with the regimen described earlier, and image analyses were performed 1 h after agent administration on day 8.

Statistical analysis

The data obtained are expressed as mean ± SEM. Differences between the test groups were analyzed by Mann–Whitney tests, Wilcoxon matched-pairs tests, or unpaired *t*-test using

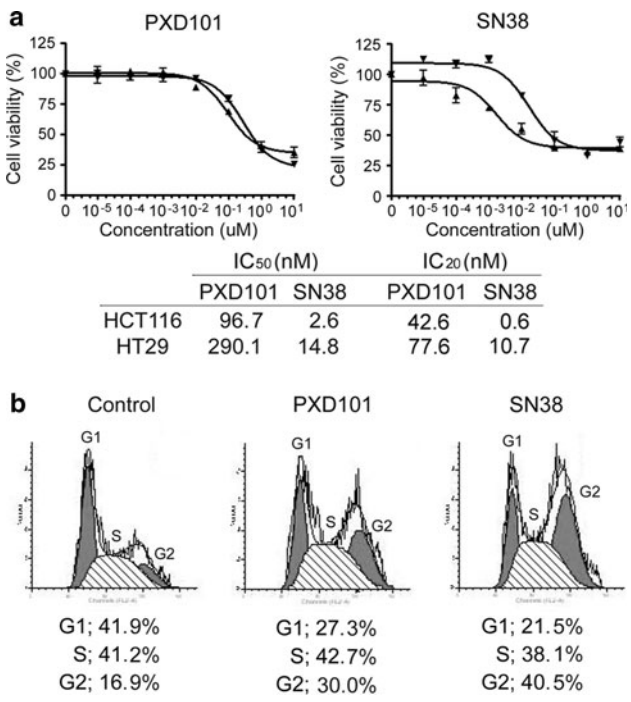

Fig. 1 Effects of PXD101 and SN38 in HCT116 and HT29 colon cancer lines. **a** IC_{50} and IC_{20} of PXD101 and SN38 alone in HCT116 and HT29 cells. **b** Cell-cycle analyses in HCT116 cells. Assays were performed at 48 h after exposure to PXD101 or SN38

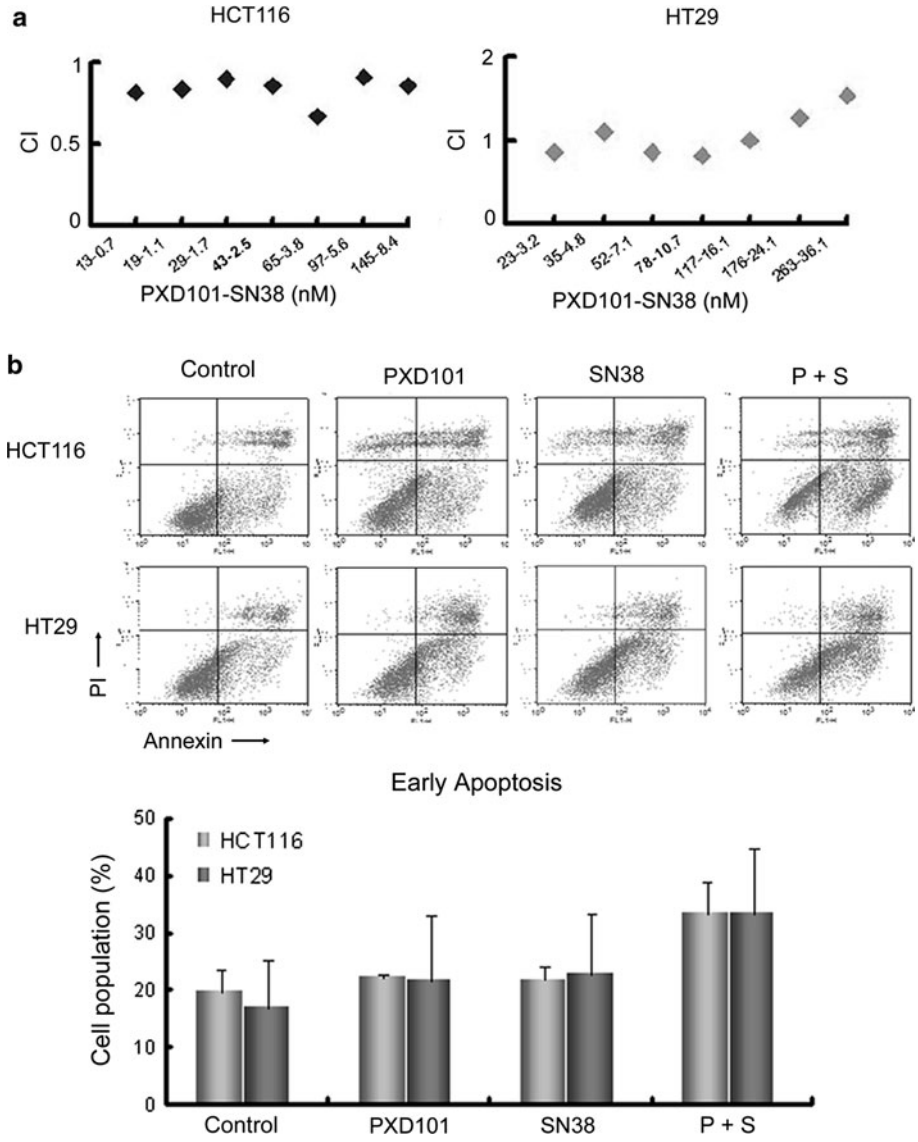

Fig. 2 Effects of PXD101 and SN38 alone and in combination at IC_{20} concentrations in colon cancer lines. **a** Combination index (*CI*) for the interaction of PXD101 and SN38 was determined in HCT116 and HT29 cells. **b** Apoptosis was induced by PXD101 and/or SN38 at IC_{20}. *Top* Representative apoptotic cells are distributed as early apoptosis (Annexin V^+ and PI^-) and late apoptosis (Annexin V^+ and PI^+). *Bottom* Percent of cell population in early apoptosis (mean ± SEM) for HCT116 and HT29 cells treated with agents, displayed as a histogram. *P* + *S*, PXD101 and SN38

GraphPad InStat (Graphpad Software). *P*-values less than 0.05 were considered statistically significant.

Results

PXD101 and SN38 possess antiproliferative activity against human colon cancer cells

To investigate the antiproliferative capacity of PXD101 and SN38 against colon cancer cells, we treated HCT116 and HT29 cells individually with various concentrations of each of the two agents for 48 h. As shown in Fig. 1a, the IC_{50} values for PXD101 or SN38 alone in HCT116 and HT29 cell lines were determined. These results indicate that both PXD101 and SN38 exerted dose-dependent anti-proliferative effects on both cell lines, but the HCT116 cell line was more sensitive to both PXD101 and SN38 than the HT29 cell line.

To evaluate the cell-cycle effects of PXD101 and SN38 in HCT116 cells, we exposed HCT116 cells to IC_{50} concentrations of PXD101 or SN38 for 48 h. PXD101 and SN38 increased the percentage of G_2 cells to 30.0 and 40.5%, respectively, compared with control cells (Fig. 1b). These data show that these two agents induced growth arrest at the G_2 phase of the cell cycle in HCT116 cells.

PXD101 and SN38 combine to synergistically affect cytotoxicity and apoptosis in colon cancer cell lines

To evaluate the combined effect of PXD101 and SN38 in HCT116 and HT29 cell lines, we first treated cells with PXD101 or SN38 alone or in combination at various doses, including IC_{20} values, and then measured cell viability

(Fig. 2a). In HCT116 cells, the combined effects of PXD101 and SN38 were greater than predicted by an additive model, indicating synergy. Synergy between PXD101 and SN38 was also evident at IC_{20} values in HT29 cells. Collectively, these results indicate that PXD101 and SN38 acted synergistically to induce enhanced cytotoxicity in colon cancer cell lines.

Next, we examined the combined effects of PXD101 and SN38 at IC_{20} concentrations on induction of apoptosis (Fig. 2b). In HCT116 cells exposed to PXD101 or SN38 alone, the percentages of early apoptotic cells were approximately 22.1 and 21.6%, respectively, compared to 19.7% in controls. In contrast, about 33.4% of HCT116 cells treated with the combination of PXD101 SN38 showed evidence of early apoptosis. Similar results were obtained in HT29 cells. Therefore, combined exposure to PXD101 and SN38 was more effective than exposure to each agent individually in both cell lines.

Combined treatment with PXD101 and SN38 exerts time- and dose-dependent effects on the expression of XIAP protein, especially in HCT116 cells

To determine the effect of single and combined treatment on the expression of acetyl-H3, H3, p21, and XIAP over time (Fig. 3a) and with different doses of each agent (Fig. 3b), we performed Western blotting in both cancer cells. The time- and dose-dependent effect of PXD101 on acetylated histone H3 levels was evident in both cancer cells. However, effect is more sensitive in the HCT116 cells.

HDACIs or irinotecan are known to be associated with induction of p21 [24–27]. Therefore, to explore whether PXD101 and SN38 combine to exert a synergistic effect on p21 expression, we performed Western blotting for p21. Both PXD101 and SN38 alone induced a time- and dose-dependent slightly increase in p21 levels in HCT116 and HT29 cells; however, there was no evidence for a synergistic effect of the two agents in combination.

We analyzed the expression of XIAP as a representative antiapoptotic protein [28]. After treating HCT116 cells with combined treatment for 8 h, XIAP expression was reduced compared to treatment with either agent alone. In HT29 cells, combined treatment for 8 h did not significantly reduce XIAP levels. However, at higher concentrations, combined treatment reduced XIAP expression in HT29 cells. These results indicate that combined treatment exerts a time- and dose-dependent effect on XIAP expression in colon cancer cells, an effect that is more prominent in the HCT116 cell line.

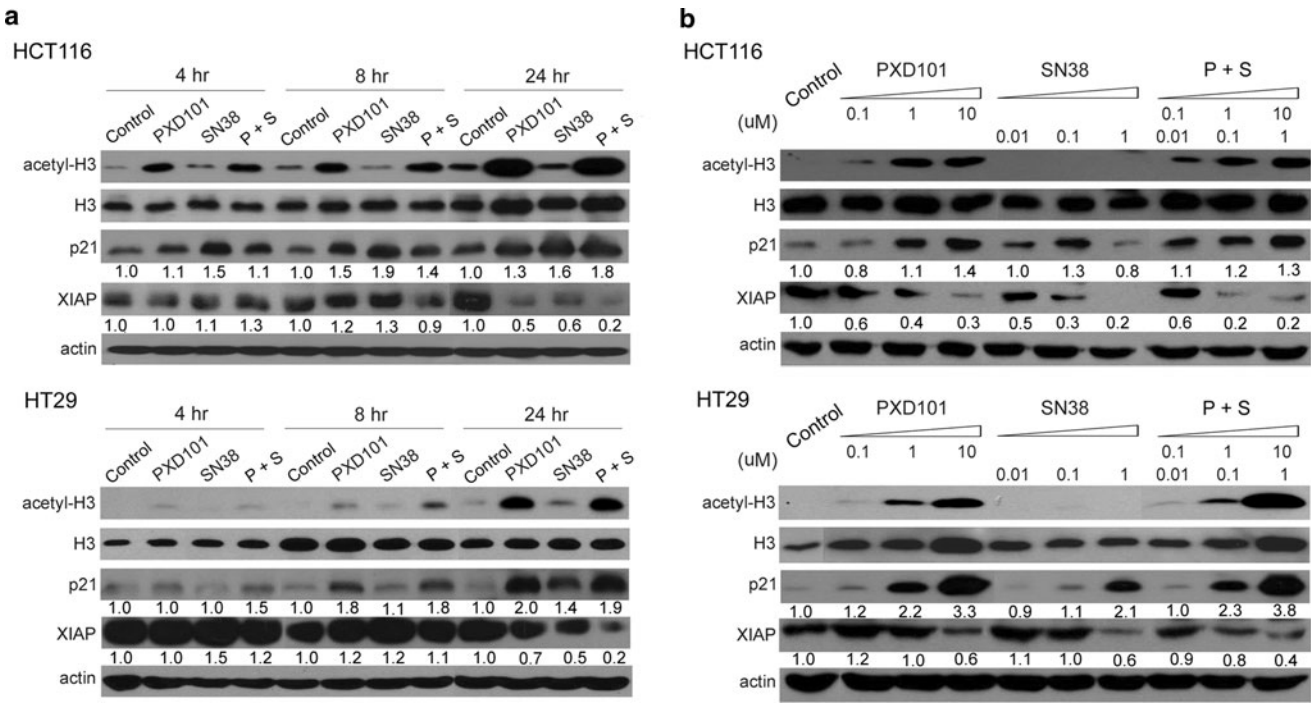

Fig. 3 Effects of PXD101 and/or SN38 on the expression of acetyl-H3, H3, p21, and XIAP in HCT116 and HT29 cells according to time (**a**) and dose (**b**). Western blotting was performed after treatment with 1 μM PXD101 and/or 0.1 μM SN38 for 4, 8, and 24 h and with 0.1, 1, 10 μM PXD101 and/or 0.01, 0.1, 1 μM SN38 for 6 h in HCT116 cells, and 22 h in HT29 cells. The ratio of p21 or XIAP:actin expression compared to control is shown for each *lane*. *P + S*, PXD101 and SN38

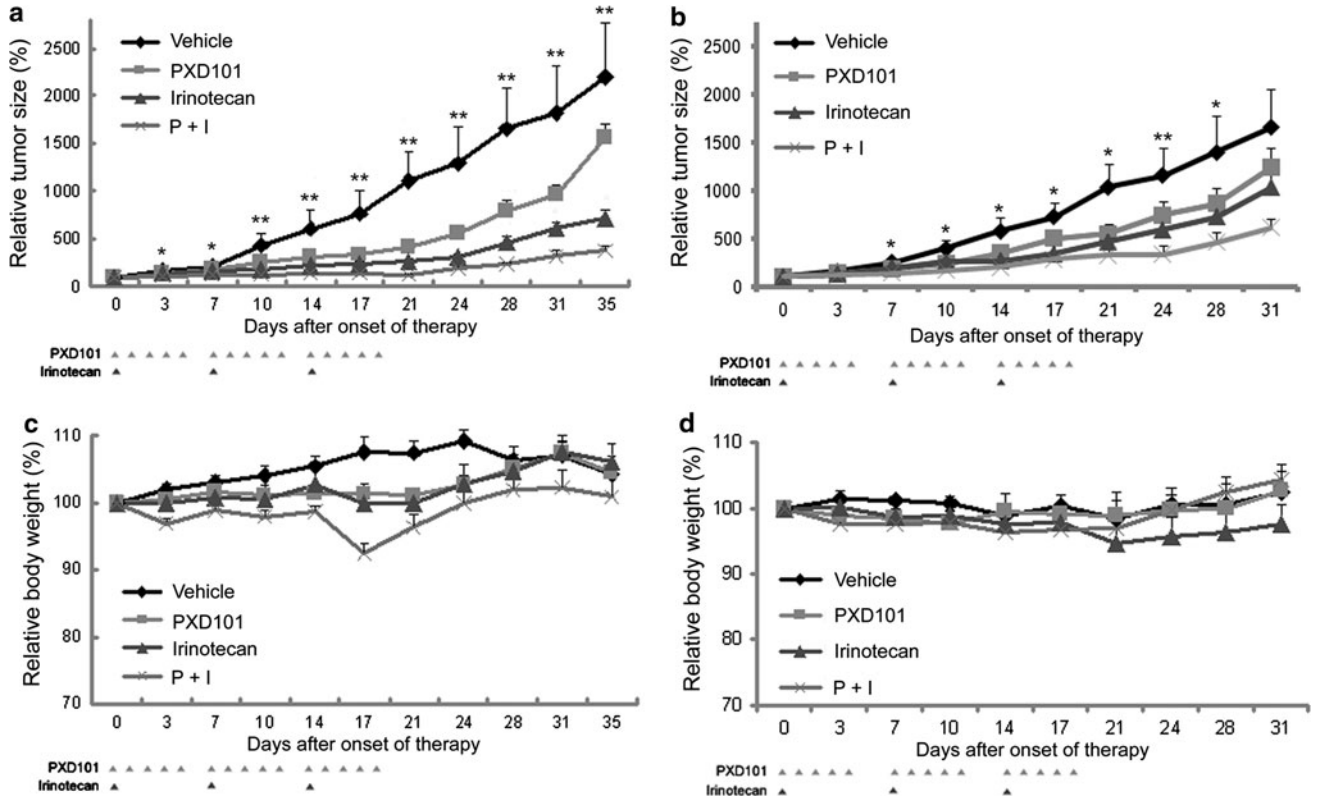

Fig. 4 Antitumor effects of PXD101 alone or in combination with irinotecan in HCT116 and HT29 xenografts. Relative tumor growth (**a**) and body weight (**c**) in HCT116 xenografts (vehicle, $n = 8$; PXD101, $n = 11$; irinotecan, $n = 7$; P + I, $n = 8$). P + I, PXD101 and irinotecan. Relative tumor growth (**b**) and body weight (**d**) in HT29 xenografts (vehicle, $n = 5$; PXD101, $n = 6$; irinotecan, $n = 6$; P + I, $n = 7$). In vivo experimental schedule of PXD101 and irinotecan are indicated at the bottom of each graph. Statistical analyses of the effects of agents on tumor size were performed using Mann–Whitney tests (*$P < 0.05$, combination vs. vehicle; **$P < 0.05$, combination vs. agents alone)

Combined administration of PXD101 and irinotecan more effectively inhibits the growth of HCT116 tumor xenografts than either agent alone

To determine whether the combination of PXD101 with irinotecan also acts synergistically in vivo, we evaluated the antitumor effect of combined treatment against HCT116 and HT29 xenografts. Combined treatment was significantly more effective in suppressing the growth of HCT116 tumors than either agent alone (Fig. 4a). In HCT116 xenografts, tumor growth was inhibited by 62.9, 75.6, and 88.2% at day 21 after treatment with PXD101 alone, irinotecan alone, and combined PXD101/irinotecan, respectively ($P < 0.01$ for combination vs. PXD101 or irinotecan). In HT29 xenografts, there was a tendency toward increased effectiveness of combined treatment, although this difference did not reach statistical significance (Fig. 4b). Thus, consistent with the in vitro findings, HT29 xenografts were less sensitive to these agents than HCT116 xenografts. Body weight was not significantly different among colon cancer cell xenograft recipients in the different treatment groups (Fig. 4c, d).

Combined treatment with PXD101 and irinotecan showed enhanced effects on HCT116 xenografts in TUNEL and colony-forming assays

To evaluate the apoptotic effects of agents on xenograft tumors, the percentage of apoptotic cells was determined (Fig. 5a). There was a modest increase in apoptosis with time after treatment with either agent alone. However, the combination treatment induced a clear increase in apoptosis above this level, indicating that combined treatment was more effective by this measure than either agent alone.

The antiproliferative activity of combined treatment and treatment with either agent alone in HCT116 xenograft tumors was assessed using a soft agar colony-formation assay (Fig. 5b). Combined treatment, and treatment with PXD101 alone, inhibited colony formation on day 16 by 87 and 50%, respectively, compared with the vehicle-treated group.

To examine the acetylation status after treatment with either agent alone or in combination, we analyzed proteins extracted from xenograft tumors on days 2 and 16 by Western blotting (Fig. 5c). Combined treatment, and treatment

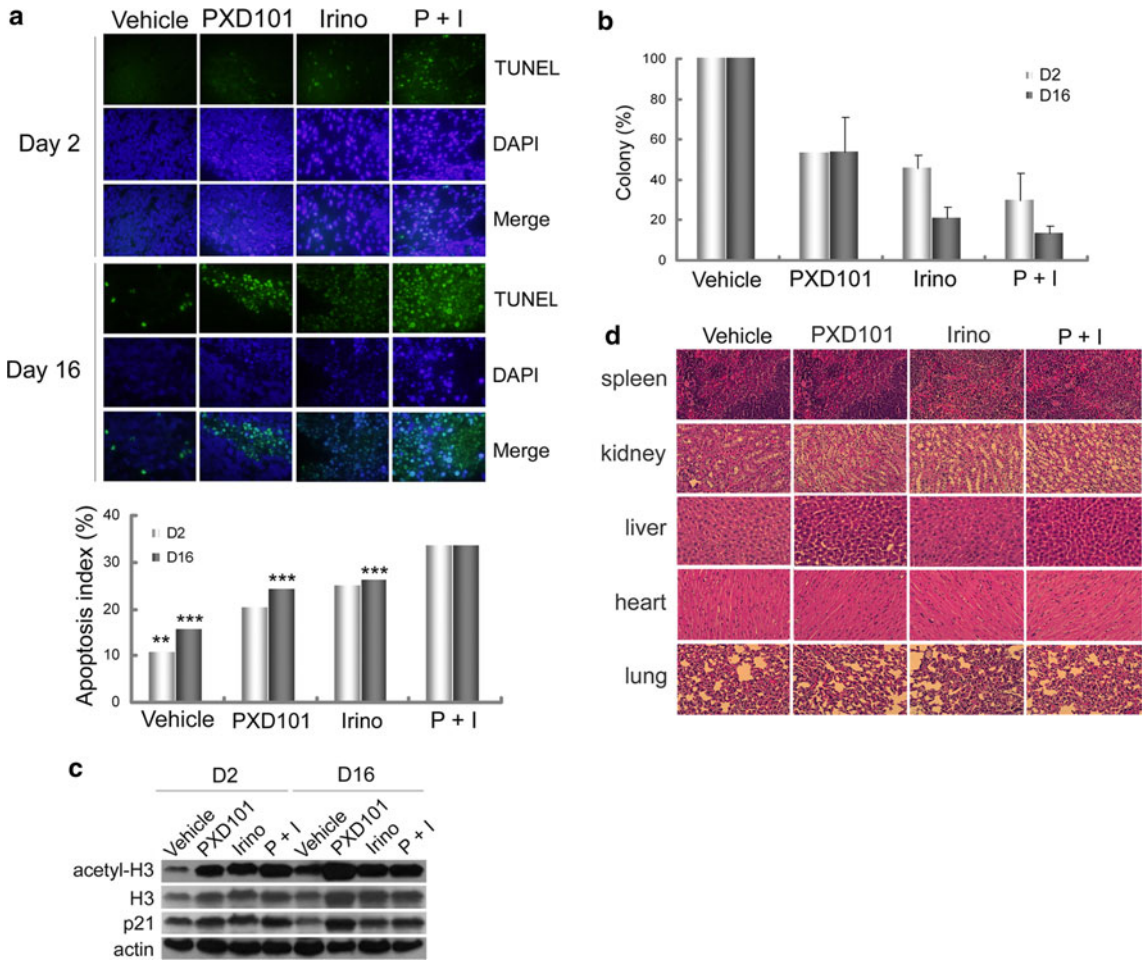

Fig. 5 Analysis of the effects of agents on HCT116 tumor xenografts. **a** Apoptosis in tumors from HCT116 xenografts treated with agents was analyzed by TUNEL assay on days 2 and 16. *Top* Representative tumor sections at the indicated times showing apoptotic cells (× 1,000). *Bottom* Apoptotic index calculated as the percentage of apoptotic cells among DAPI-stained cells. Unpaired *t*-test; $^{**}P < 0.01$ versus combination; $^{***}P < 0.001$ versus combination. **b** The effects of PXD101 and/or irinotecan on the survival of tumor cells in HCT116 xenografts were analyzed using a soft agar colony-forming assay. **c** The acetylation of H3 and induction of p21 in xenograft tumors were analyzed by Western blotting on days 2 and 16 after agent treatment. **d** Organs from HCT116 xenograft-bearing mice treated with agents were H&E-stained

with PXD101 alone, increased H3 acetylation on day 16. Moreover, each agent alone and both agents in combination induced p21 expression. Potential additive toxic effects of PXD101 and irinotecan on organs were assessed by hematoxylin-eosin staining (Fig. 5d). A histologic analysis of organs (lung, liver, spleen, kidney, and heart) of xenografted mice after treatment with both agents showed no evident tissue damage.

[^{18}F]FLT-PET can detect early responses to PXD101 and irinotecan in HCT116 tumor-bearing mice

HDACIs and irinotecan alone are known to decrease the expression of TK1 [29, 30], which can be inferred from PET imaging of [^{18}F]FLT uptake. To assess whether [^{18}F]FLT-PET imaging is able to detect early responses to PXD101 and irinotecan in colon cancer and reveal potential synergies, we imaged xenografts with [^{18}F]FLT-PET on day 0 and again 8 days after administration of agents (Fig. 6a). [^{18}F]FLT uptake (mean SUVs), which was increased by 136.5% in vehicle-treated tumors, was decreased or unchanged after treatment with agents (Fig. 6b). Specifically, irinotecan alone and the combined treatment significantly decreased mean SUVs by 55.2 and 63.7%, respectively. These results indicate that [^{18}F]FLT-PET may detect early responses to PXD101 and irinotecan, and suggest that [^{18}F]FLT-PET can serve as an imaging biomarker for predicting responses to these agents in patients with colon cancer. However, under the conditions used, we were unable to detect a synergistic effect of the combined treatment by [^{18}F]FLT-PET.

After analysis of PET images on day 8, we analyzed the level of TK1 expression in HCT116 xenograft tumors from agent-treated mice by Western blotting. The combination

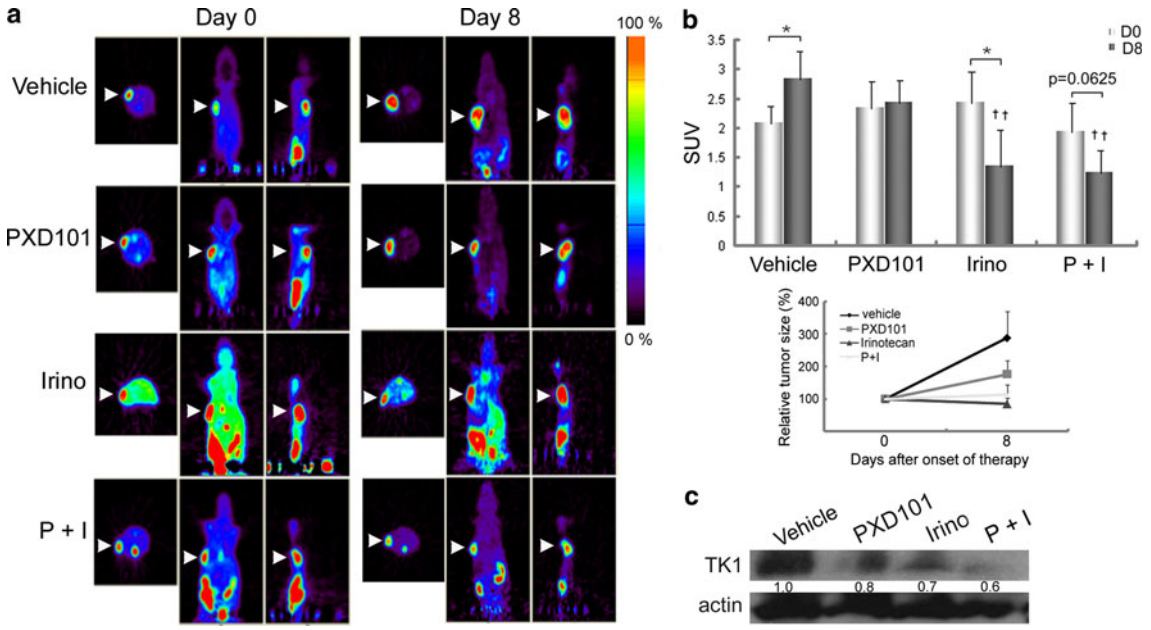

Fig. 6 [^{18}F]FLT-PET analysis of HCT116 xenografts after administration of PXD101 and/or irinotecan (Irino). **a** Representative [^{18}F]FLT-PET images of HCT116 xenografts 0 and 8 days after treatment with agents are displayed. Note color bar. *Arrows*, tumors. **b** Quantitative analysis of [^{18}F]FLT-PET expressed as the mean ± SD ($n = 6$) of standardized uptake value (SUV). $^{*}P < 0.05$ for D0 versus D8 by Wilcoxon matched-pairs test; $^{\dagger\dagger}P < 0.01$ for vehicle versus agents on D8 by Mann–Whitney test. *Bottom* Relative tumor growth. **c** TK1 expression in HCT116 xenograft tumors analyzed by Western blotting on day 8 after administration of agents. The ratio of TK1:actin expression compared to control is shown for each *lane*

treatment showed a decrease in TK1 protein level compared to each agent alone (Fig. 6c).

Discussion

In this study, we demonstrated that combined treatment with PXD101 and irinotecan produces enhanced antitumor effects in colon cancers compared to treatment with either agent alone. Because irinotecan-based regimens are used broadly for the treatment of colon, gastric, and small-cell lung cancer, strategies to improve the efficacy of irinotecan are of significant clinical importance. To the best of our knowledge, this is the first report that HDACIs synergize with irinotecan to enhance the antitumor efficacy of irinotecan in colon cancer in vitro as well as in vivo.

Several in vitro studies have examined the combination of HDACIs and irinotecan in gastrointestinal (GI) malignancies. Piacentini et al. reported that the combination of Trichostatin A (TSA) and irinotecan inhibited the growth of pancreatic cancer cell lines by 80% [31]. Zhang et al. also reported that the combination of TSA with SN38 exerted a synergistic antiproliferative effect in gastric cancer cell lines [32]. Similarly, we showed in a previous in vitro study that some HDACIs, including suberoylanilide hydroxamic acid (SAHA), synergized with a folinic acid, fluorouracil, and irinotecan (FOLFIRI) regimen in cultured colorectal cancer cells [15]. Consistent with these studies, we showed here that combined treatment with PXD101 and irinotecan exerted antitumor effects in colon cancer. Taken together, these data provide a rationale for a novel therapy in patients with GI cancers, including colon cancer. Combination therapies for human tumors using HDACIs and irinotecan are currently under active investigation [35].

Few studies have investigated the precise mechanisms underlying the synergy between HDACIs and irinotecan. It has been suggested that because HDACIs induce acetylation of histone and thereby loosens the chromatin structure, topoisomerase inhibitor may more easily access DNA, thereby facilitating DNA damage [11, 33, 34]. Irinotecan combined with HDACIs may also significantly enhance the level of ATM (ataxia-telangiectasia-mutated) leading to apoptosis: irinotecan activates ATM and Chk2 and then induces apoptosis [36], and besides HDACIs regulate DNA damage responses, including activation of ATM, and thereby induce apoptosis [37]. Further studies are needed to establish the validity of these hypothetical explanations for the synergistic effects of HDACI and irinotecan combinations.

In the present study, HCT116 cells were significantly more susceptible to PXD101 than were HT29 cells both in vitro and in vivo, in line with previous observations [38]. LaBonte et al. have analyzed the gene expression profiles that accompany treatment with the HDACIs SAHA and LBH589 in these two cell lines. Notably, they observed

significant cell-line-specific alterations in genes involved in angiogenesis, mitosis, and apoptosis. These different alterations might explain the differential sensitivities of HCT116 and HT29 cell lines to HDACIs, a supposition that should be validated in further studies.

The discovery of appropriate biomarkers is crucial in the preclinical and clinical development of new anticancer agents. There are currently no established biomarkers for HDACIs. Recently, Leyton et al. showed that the HDACI LAQ824 decreased tumor [^{18}F]FLT-PET uptake in HCT116 colon carcinoma xegongrafts [29]. They also revealed that the change in tumor [^{18}F]FLT-PET uptake was due to a reduction in TK1 transcription and translation. In the present study, PXD101 treatment either prevented an increase in [^{18}F]FLT uptake (PXD101 alone) or decreased [^{18}F]FLT uptake (in combination with irinotecan). These treatments also reduced TK1 levels in tumor xenografts compared with those in vehicle-treated mice. Taken together, these data suggest the utility of [^{18}F]FLT-PET for monitoring the biological activity of HDACIs. Further studies are needed to confirm the value of this non-invasive imaging biomarker to monitor the biological activities of HDACIs.

There are some limitations to the present study. First, in contrast to combination index results, we did not observe a synergistic antitumor effect of PXD101 in combination with irinotecan in colon xenografts. This might be due to tumor microenvironment. Microenvironmental factors such as blood vessels, the extracellular matrix, cytokines, and growth factors on the action of these agents can affect the sensitivity of tumor cells [39, 40]. Hypoxia region and acidity of solid tumor can influence the action of these agents [41–43]. In addition, HDACIs can have various effects on many genes which may affect both the tumor cells and their microenvironment. Thus, effects of these agents under these complex microenvironments seem to be weaker than in in vitro. Another limitation of this study is only one dose of these agents, selected on the basis of previous reports [44], was administered. Thus, it is possible that the use of several doses, including lower doses, might have revealed synergistic effects.

In conclusion, our studies show that the combination of PXD101 and irinotecan might be a promising therapeutic regimen for the treatment of colon cancer and provide support for clinical trials of PXD101 and irinotecan combinations.

Acknowledgments This study was supported by grants from the Korea Health 21 R&D Project, Ministry of Health, Welfare, and Family Affairs, Republic of Korea (A062254).

Conflicts of interest None declared.

References

1. Jemal A, Siegel R, Ward E, Hao Y, Xu J et al (2009) Cancer statistics, 2009. CA Cancer J Clin 59:225–249
2. Kohne CH, Lenz HJ (2009) Chemotherapy with targeted agents for the treatment of metastatic colorectal cancer. Oncologist 14:478–488
3. Weekes J, Lam AK, Sebesan S, Ho YH (2009) Irinotecan therapy and molecular targets in colorectal cancer: a systemic review. World J Gastroenterol 15:3597–3602
4. Teicher BA (2008) Next generation topoisomerase I inhibitors: rationale and biomarker strategies. Biochem Pharmacol 75:1262–1271
5. Marks PA, Xu WS (2009) Histone deacetylase inhibitors: potential in cancer therapy. J Cell Biochem 107:600–608
6. Knupfer MM, Pulzer F, Schindler I, Hernaiz Driever P, Knupfer H et al (2001) Different effects of valproic acid on proliferation and migration of malignant glioma cells in vitro. Anticancer Res 21:347–351
7. Witt O, Monkemeyer S, Kanbach K, Pekrun A (2002) Induction of fetal hemoglobin synthesis by valproate: modulation of MAP kinase pathways. Am J Hematol 71:45–46
8. Yuan PX, Huang LD, Jiang YM, Gutkind JS, Manji HK et al (2001) The mood stabilizer valproic acid activates mitogen-activated protein kinases and promotes neurite growth. J Biol Chem 276:31674–31683
9. Wilson AJ, Byun DS, Popova N, Murray LB, L'Italien K et al (2006) Histone deacetylase 3 (HDAC3) and other class I HDACs regulate colon cell maturation and p21 expression and are deregulated in human colon cancer. J Biol Chem 281:13548–13558
10. Nakagawa M, Oda Y, Eguchi T, Aishima S, Yao T et al (2007) Expression profile of class I histone deacetylases in human cancer tissues. Oncol Rep 18:769–774
11. Mariadason JM (2008) HDACs and HDAC inhibitors in colon cancer. Epigenetics 3:28–37
12. Nian H, Bisson WH, Dashwood WM, Pinto JT, Dashwood RH (2009) Alpha-keto acid metabolites of organoselenium compounds inhibit histone deacetylase activity in human colon cancer cells. Carcinogenesis 30:1416–1423
13. Buggy JJ, Cao ZA, Bass KE, Verner E, Balasubramanian S et al (2006) CRA-024781: a novel synthetic inhibitor of histone deacetylase enzymes with antitumor activity in vitro and in vivo. Mol Cancer Ther 5:1309–1317
14. Fazzone W, Wilson PM, Labonte MJ, Lenz HJ, Ladner RD (2009) Histone deacetylase inhibitors suppress thymidylate synthase gene expression and synergize with the fluoropyrimidines in colon cancer cells. Int J Cancer 125:463–473
15. Kim JC, Shin ES, Kim CW, Roh SA, Cho DH et al (2009) In vitro evaluation of histone deacetylase inhibitors as combination agents for colorectal cancer. Anticancer Res 29:3027–3034
16. Prince HM, Bishton MJ, Harrison SJ (2009) Clinical studies of histone deacetylase inhibitors. Clin Cancer Res 15:3958–3969
17. Stimson L, La Thangue NB (2009) Biomarkers for predicting clinical responses to HDAC inhibitors. Cancer Lett 280:177–183
18. Salskov A, Tammisetti VS, Grierson J, Vesselle H (2007) FLT: measuring tumor cell proliferation in vivo with positron emission tomography and 3′-deoxy-3′-[18F]fluorothymidine. Semin Nucl Med 37:429–439
19. Shields AF, Grierson JR, Dohmen BM, Machulla HJ, Stayanoff JC et al (1998) Imaging proliferation in vivo with [F-18]FLT and positron emission tomography. Nat Med 4:1334–1336
20. Rasey JS, Grierson JR, Wiens LW, Kolb PD, Schwartz JL (2002) Validation of FLT uptake as a measure of thymidine kinase-1 activity in A549 carcinoma cells. J Nucl Med 43:1210–1217

21. Chou TC, Talalay P (1984) Quantitative analysis of dose-effect relationships: the combined effects of multiple drugs or enzyme inhibitors. Adv Enzyme Regul 22:27–55
22. Chou TC, Motzer RJ, Tong Y, Bosl GJ (1994) Computerized quantitation of synergism and antagonism of taxol, topotecan, and cisplatin against human teratocarcinoma cell growth: a rational approach to clinical protocol design. J Natl Cancer Inst 86:1517–1524
23. Martin SJ, Eisenbarth JA, Wagner-Utermann U, Mier W, Henze M et al (2002) A new precursor for the radiosynthesis of [18F]FLT. Nucl Med Biol 29:263–273
24. Plumb JA, Finn PW, Williams RJ, Bandara MJ, Romero MR et al (2003) Pharmacodynamic response and inhibition of growth of human tumor xenografts by the novel histone deacetylase inhibitor PXD101. Mol Cancer Ther 2:721–728
25. Niculescu AB 3rd, Chen X, Smeets M, Hengst L, Prives C et al (1998) Effects of p21(Cip1/Waf1) at both the G1/S and the G2/M cell cycle transitions: pRb is a critical determinant in blocking DNA replication and in preventing endoreduplication. Mol Cell Biol 18:629–643
26. Rodriguez R, Hansen LT, Phear G, Scorah J, Spang-Thomsen M et al (2008) Thymidine selectively enhances growth suppressive effects of camptothecin/irinotecan in MSI+cells and tumors containing a mutation of MRE11. Clin Cancer Res 14:5476–5483
27. Liu Y, Xing H, Weng D, Song X, Qin X et al (2009) Inhibition of Akt signaling by SN-38 induces apoptosis in cervical cancer. Cancer Lett 274:47–53
28. Dai Y, Chen S, Kramer LB, Funk VL, Dent P et al (2008) Interactions between bortezomib and romidepsin and belinostat in chronic lymphocytic leukemia cells. Clin Cancer Res 14:549–558
29. Leyton J, Alao JP, Da Costa M, Stavropoulou AV, Latigo JR et al (2006) In vivo biological activity of the histone deacetylase inhibitor LAQ824 is detectable with 3′-deoxy-3′-[18F]fluorothymidine positron emission tomography. Cancer Res 66:7621–7629
30. Voeller DM, Grem JL, Pommier Y, Paull K, Allegra CJ (2000) Identification and proposed mechanism of action of thymidine kinase inhibition associated with cellular exposure to camptothecin analogs. Cancer Chemother Pharmacol 45:409–416
31. Piacentini P, Donadelli M, Costanzo C, Moore PS, Palmieri M et al (2006) Trichostatin A enhances the response of chemotherapeutic agents in inhibiting pancreatic cancer cell proliferation. Virchows Arch 448:797–804
32. Zhang X, Yashiro M, Ren J, Hirakawa K (2006) Histone deacetylase inhibitor, trichostatin A, increases the chemosensitivity of anticancer drugs in gastric cancer cell lines. Oncol Rep 16:563–568
33. Marchion DC, Bicaku E, Daud AI, Richon V, Sullivan DM et al (2004) Sequence-specific potentiation of topoisomerase II inhibitors by the histone deacetylase inhibitor suberoylanilide hydroxamic acid. J Cell Biochem 92:223–237
34. Marchion DC, Bicaku E, Turner JG, Daud AI, Sullivan DM et al (2005) Synergistic interaction between histone deacetylase and topoisomerase II inhibitors is mediated through topoisomerase IIb-eta. Clin Cancer Res 11:8467–8475
35. Fetterly GJ, Brady WE, LeVea CM, Litwin AM, Zagst PD, Prey JD, Tarquini M, Giardina MK, Iyer RV, Khushalani NI (2009) A phase I pharmacokinetic (PK) study of vorinostat in combination with irinotecan, 5-fluorouracil, and leucovorin in advanced upper gastrointestinal cancers. J Clin Oncol 27:15s (suppl; abstr e15540)
36. Takemura H, Rao VA, Sordet O, Furuta T, Miao ZH et al (2006) Defective Mre11-dependent activation of Chk2 by ataxia telangiectasia mutated in colorectal carcinoma cells in response to replication-dependent DNA double strand breaks. J Biol Chem 281:30814–30823
37. Glaser KB (2007) HDAC inhibitors: clinical update and mechanism-based potential. Biochem Pharmacol 74:659–671
38. LaBonte MJ, Wilson PM, Fazzone W, Groshen S, Lenz HJ et al (2009) DNA microarray profiling of genes differentially regulated by the histone deacetylase inhibitors vorinostat and LBH589 in colon cancer cell lines. BMC Med Genomics 2:67
39. Tredan O, Galmarini CM, Patel K, Tannock IF (2007) Drug resistance and the solid tumor microenvironment. J Natl Cancer Inst 99:1441–1454
40. Jeon HW, Lee YM (2010) Inhibition of histone deacetylase attenuates hypoxia-induced migration and invasion of cancer cells via the restoration of RECK expression. Mol Cancer Ther 9:1361–1370
41. Shen J, Hughes C, Chao C, Cai J, Bartels C et al (1987) Coinduction of glucose-regulated proteins and doxorubicin resistance in Chinese hamster cells. Proc Natl Acad Sci USA 84:3278–3282
42. Gerweck LE, Vijayappa S, Kozin S (2006) Tumor pH controls the in vivo efficacy of weak acid and base chemotherapeutics. Mol Cancer Ther 5:1275–1279
43. Raghunand N, He X, van Sluis R, Mahoney B, Baggett B et al (1999) Enhancement of chemotherapy by manipulation of tumour pH. Br J Cancer 80:1005–1011
44. Mercalli A, Sordi V, Formicola R, Dandrea M, Beghelli S et al (2007) A preclinical evaluation of pemetrexed and irinotecan combination as second-line chemotherapy in pancreatic cancer. Br J Cancer 96:1358–1367